Bhumipol Dam Operation Improvement via smart system for the Thor Tong Daeng Irrigation Project, Ping River Basin, Thailand

Sucharit Koontanakulvong [1, a*], Tran Thanh Long [2, b], Tuan Pham Van [3, c]

[1, 2,3] Dept. of Water Resources Engineering, Chulalongkorn University, Bangkok, Thailand

[a]Sucharit.k@chula.ac.th, [b]ttlongdcbk@yahoo.com, [c]phamtuanld8@gmail.com

Abstracts

The Tor Tong Daeng Irrigation Project with the irrigation area of 61,400 hectares is located in the Ping Basin of the Upper Central Plain of Thailand where farmers depended on both surface water and groundwater. In the drought year, water storage in the Bhumipol Dam is inadequate to allocate water for agriculture, and caused water deficit in many irrigation projects. Farmers need to find extra sources of water such as water from farm pond or groundwater as a supplement. The operation of Bhumipol Dam and irrigation demand estimation are vital for irrigation water allocation to help solve water shortage issue in the irrigation project.

The study aims to determine the smart dam operation system to mitigate water shortage in this irrigation project via introduction of machine learning to improve dam operation and irrigation demand estimation via soil moisture estimation from satellite images. Via ANN technique application, the inflows to the dam are generated from the upstream rain gauge stations using past 10 years daily rainfall data. The input vectors for ANN model are identified base on regression and principal component analysis. The structure of ANN (length of training data, the type of activation functions, the number of hidden nodes and training methods) is determined from the statistics performance between measurements and ANN outputs. On the other hands, the irrigation demand will be estimated by using satellite images, LANDSAT. The Enhanced Vegetation Index (EVI) and Temperature Vegetation Dryness Index (TVDI) values are estimated from the plant growth stage and soil moisture. The values are calibrated and verified with the field plant growth stages and soil moisture data in the year 2017-2018. The irrigation demand in the irrigation project is then estimated from the plant growth stage and soil moisture in the area. With the estimated dam inflow and irrigation demand, the dam operation will manage the water release in the better manner compared with the past operational data.

The results show how smart system concept was applied and improve dam operation by using inflow estimation from ANN technique combining with irrigation demand estimation from satellite images when compared with the past operation data which is an initial step to develop the smart dam operation system in Thailand.

Keywords: dam operation, ANN, irrigation demand, satellite images, smart system, Bhumipol Dam,

Thor Thong Daeng Irrigation, Thailand

1. Introduction

The long-standing strategy of a dam is to impound water for securing a reliable source of water for a wide variety of human and environmental needs, especial in developing countries. Traditionally, the dam operates under the operator's subjective judgments thoroughly on stationarity and past hydrological experience by heuristics procedures and rule curves (Celeste and Billib 2009; Rittima 2009; Ehsani et al. 2017). Furthermore, the frequency of extreme floods and droughts have been increasing more than before (Huntington 2006). Thus, the decision making of release becomes more challenge under the effects of both climate variability and human responses during extreme water years. Although the optimal reservoir's rule curves has extensively approach over the last few decades such as dynamic programing (DP) (Chaleeraktrakoon and Kangrang 2007), genetic algorithms (GAs) (Tospornsampan et al. 2005), simulated annealing (SA) algorithms (Lamom, Thepchatri, and Rivepiboon 2008), the reservoir operating system has not been provided a comprehensive solution for multi-objective in real-world problems. Besides, the prediction of real-time dam inflows still remains obstacle in effective transmission of precipitation information, consuming computation time and memory capacity (Kim, Heo, and Jeong 2006).

Nowadays, the development of optimum irrigation has been becoming more and more important with a primary role of controlling rate and time of irrigation water to meet crop water demand, while constraining losses and preserving water resources (Alhammadi and Al-Shrouf 2013). The soil layer and actual value of soil moisture content (SMC) at any given time must be known before any decisions on improving irrigation management can be made. In recent years, satellite surface soil moisture has tended to be more widely available (Champagne et al. 2016). A water content map can be created, with the classification of the high, medium, and low water-content areas (GISTDA) by calculating indices from multispectral satellite images from visible (red band) and infrared bands (near infrared and thermal bands) (Potić, Bugarski, and Matić-Varenica 2017). In which, Temperature Vegetation Dryness Index (TVDI) presents as an indicator of soil moisture in agricultural areas on both local and regional scales (Chen et al. 2015; Schirmbeck 2017; Gao, Gao, and Chang 2011).

2. Objectives and scope

The study aims to determine the smart dam operation system to mitigate water shortage in this irrigation project via introduction of machine learning to improve dam operation and irrigation demand estimation via soil moisture estimation from satellite images. Via ANN technique application, the inflows to the dam are generated from the upstream rain gauge stations using past 10 years daily rainfall data. The input vectors for ANN model are identified base on regression and principal component analysis. The structure of ANN (length of training data, the type of activation functions, the number of hidden nodes and training methods) is determined from the statistics performance between measurements and ANN outputs. On the other hands, the irrigation demand will be estimated by using satellite images, LANDSAT. The Enhanced Vegetation Index (EVI) and Temperature Vegetation Dryness Index (TVDI) values are estimated from the plant growth stage and soil moisture. The values are calibrated and verified with the field plant growth stages and soil moisture data in the year 2017-2018. The irrigation demand in the irrigation project is then estimated from the plant growth stage and soil moisture in the area. With the estimated dam inflow and irrigation demand, the dam operation will manage the water release in the better manner compared with the past operation figures in the Ping Basin as shown in Figure 1.

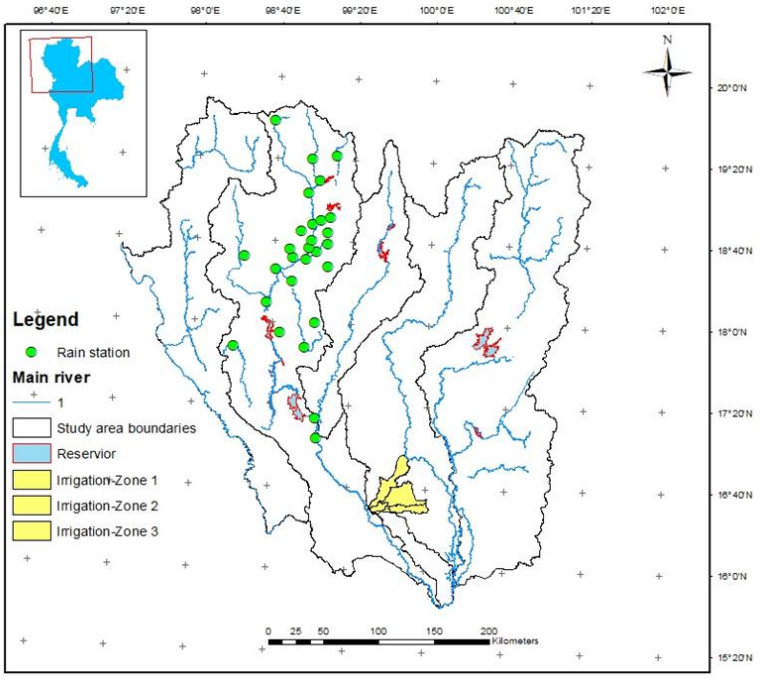

Figure 1 Study area

The inputs for rainfall runoff model was obtained daily precipitation of 33 stations from RID, HAII, and TMD during the year 2009-2018. The rainfall of selected station corresponds with inflow pattern at the dam. The maximum distance from the dam to rainfall station is 200km. The daily inflow of Bhumipol Dam was utilized to calibrate and validate in rainfall runoff process. The daily reservoir storage capacity of the dam was input data for dam release simulation.

3. Methods used

There are three packages in the study system to better the dam operation, i.e., inflow package, release package and irrigation demand package.

a) Inflow package

Since ANN with one hidden layer is sufficient to solve all problem of the hydrologic process (Kolmogorov 1957; De Vos and Rientjes 2005), the architecture of each ANN for hydrology process model consists one input layer, one hidden layer, and one output layer. In the training process, the interconnected each neuron in hidden layer received signals from the input units through weight connectors and biases, then transformed towards the output neuron using log sigmoid activation function. Since the appropriate number of dependent nodes for hidden layer is unknown, a trial and-error method was adapted to find the best network's configuration (number of nodes, weights, biases). The training network was selected through the best performance of fitting among the neural network predicted values and the desired outputs. The linear function was employed as transfer function for ANN because the linear function is known to be robust for a continuous output variable. The training of the neural network models was stopped when either the goal of error was achieved or the number of iterations exceeded a prescribed value.

The antecedent precipitation, moving mean rainfall, previous inflow is common potential input to enhance forecasting ability in the updating case of rainfall – runoff ANN model (Rajurkar, Kothyari, and Chaube 2004). Thus, the suitable input variables and proper hidden neutrons of ANN were identified from 6 combinations of input variables by virtue of statistic performance (MSE, R^2) as follows: **C1:** *R*(*t*-1), *I*(*t*-1); **C2:** *R*(*t*-1), $MR_{(30\ days)}$; **C3:** *R*(*t-1*),*I*(*t-1*), *I*(*t-2*); **C4:** *R*(*t*-1), *R*(*t*-2), *I*(*t*-1), *I*(*t*-2); **C5:** *R*(*t*-1), $MR_{(30\ days)}$,*I*(*t*-1), *I*(*t*-2); **C6:** *R*(*t*-1),*R*(*t*-2), $MR_{(30\ days)}$, *I*(*t*-1). Where R means rainfall; MR is moving average; I presents inflow at the dam

b) Dam Release Package

For dam release modeling, the inflow and the capacity from previous time steps are commonly inputs for dam operation modeling (Ehsani et al. 2016). To define the proper input variables and hidden neutrons of ANN, six combinations of input variables was evaluated performance training by statistic (MSE, R^2) as follows: **D1:** R(t-1), C(t-1); **D2:** R(t-1), C(t-1), I(t-1); **D3:** R(t-1), R(t-2), C(t-1), I(t-1); **D4:** R(t-1), C(t-1), C(t-2), I(t-1); **D5:** C(t-2), C(t-1), I(t-1), I(t-2); **D6:** R(t-1), C(t-1), C(t-2), I(t-1), I(t-2). Where C means reservoir capacity.

c) Irrigation Demand Package

The main objective of this study was to improve water management based on plant growth and soil moisture during dry season by applying satellite images. The crop information and statistical reports extracted from satellite imagery were integrated with field data and collateral data and the results were analyzed on GIS platform. Figure 2 describes the framework of plant growth and soil moisture estimation and their application.

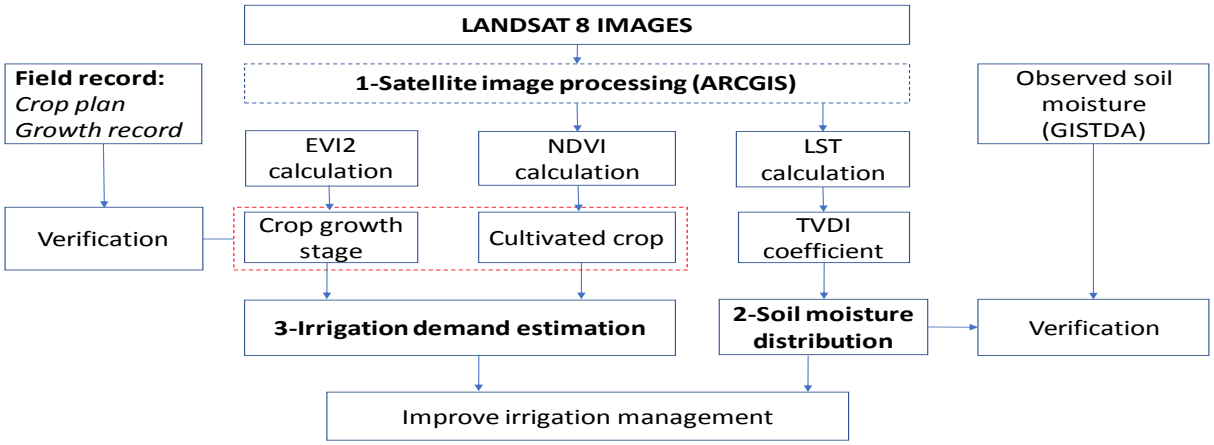

Figure 2 - Framework of the irrigation demand method

Landsat 8 images acquisition

Landsat 8 OLI (Operational Land Imager) and TIRS (Thermal Infrared Sensor) images are free and have Thermal Infrared (TIRS) bands (Band 10 and 11, 100 m spatial resolution resampled to 30 meter) that can be used for soil moisture estimation with good spatial resolution. Nineteen multi-date LANDSAT are used for this study. The images were rectified and geo-referenced to the WGS 84 datum on the UTM coordinate system (Zone 47N)

Preprocessing

The enhanced vegetation index (EVI) was developed to optimize the vegetation signal with improved sensitivity in high biomass regions and improved vegetation monitoring through a de-coupling of the canopy background signal and a reduction in atmosphere influences. Under clear sky conditions, the SWIR spectral bands are highly correlated with the visible (blue, green and red) spectral bands over various land covers (Kaufman et al. 2001). A 2-band EVI (EVI2) (Equation below) without a blue band is developed and evaluated using global, land cover specific, and local scale satellite data (Jiang et al. 2008).

$$EVI2 = 2.5\frac{NIR - RED}{NIR + 2.4RED + 1}$$

The Normalized Differential Vegetation Index (NDVI) is a standardized vegetation index which Calculated using Near Infra-red (Band 5) and Red (Band 4) (Tucker 1979) shown in equation below:

$$NDVI = \frac{NIR - RED}{NIR + RED}$$

The linear combination of Normalized Differential Vegetation Index (NDVI) - Land Surface Temperature (LST) typically shows a strong negative relationship and the Temperature Vegetation Dryness Index (TVDI) can be estimated from the dry and wet edges of the triangle (Sandholt, Rasmussen, and Andersen 2002). In the feature space, TVDI is also computed based on information about the wet edge representing the minimum LST (LSTmin, maximum evaporation and thereby, unlimited water access) as straight line parallel to the NDVI axis. Therefore, the TVDI is related to soil moisture status is high values indicating dry conditions and low values indicate moist conditions. The TVDI of each pixel can be defined using equation below:

$$TVDI = \frac{LST - LST_{smin}}{LST_{smax} - LST_{smin}}$$

Where the land surface temperature (LST) is the temperature of the Earth's surface as derived from remotely sensed thermal infrared data (Weng, Fu et al. 2014). The Landsat 8 LST was computed by fusing images of MODIS LST and Landsat 8 brightness temperature (T_b), provided by Hazaymeh and Hassan (2015).

$$LST = (BT / 1) + W * (BT / 14380) * \ln(E)$$

Where BT is Top of atmosphere brightness temperature (℃), W = Wavelength of emitted radiance and E = Land Surface Emissivity

Soil moisture content estimation

A soil moisture estimation model is established by using a collection of soil moisture observation and remote sensing data. A stepwise multiple regression approach was used to assess the relationship between observed soil moisture data and remote sensing data, i.e., TVDI were used as independent variables. The model can be computed by a regression formula as follows:

$$\text{Estimated soil moisture} = a + b(TVDI)$$

Where, the estimated soil moisture is given as a percentage (%), and a, b are the coefficients of the regression lines of the TVDI.

Irrigation demand estimation

Crop water demand are defined here as "the depth of water needed to meet the water loss through evapotranspiration (ET_{crop}) of a disease-free crop, growing in large fields under non-restricting soil conditions including soil water and fertility and achieving full production potential under the given growing environment". This water can be supplied to the crops in various ways such as by rainfall, irrigation or a combination of irrigation and rainfall. In this study area, part of the crop water need is supplied by rainfall and the remaining part by irrigation. In such cases, the irrigation water demand is the difference between the crop water need (ET crop) and that part of the rainfall which is effectively used by the plants (Pe). In formula:

$$IWD = ET_{crop} - Pe = Kc*ET_o - Pe$$

where Pe is effective rainfall and ET_o is reference crop evapotranspiration which can calculated based a three-stage procedure of Allen et al. (1998). Besides, total water demand of irrigation area can be estimated by using EVI2 coefficient to define growth stage and NDVI to distribute crop area.

4. Results

a) Inflow package

The ANN with a combination of previous rainfall and two consecutive days of inflow presented the best performance. The structure consists of 14 neurons in its hidden layer. The RMSE of calibration and validation are 6.99 mcm, and 6.0 mcm, respectively. The R^2 of calibration and validation are 0.92 and 0.9, respectively. Although, the output of ANN model C4 showed agreement with target inflow, its fail to simulate peak flow (Figure 3a). The rainfall input was obtained from 33 stations, so it is unsurprisingly that ANN network was become complex with many redundant weights and caused inadequate outputs. To illuminate this problem, the precipitation was connected to conveniently input layer before transfer to hidden layer (see Figure 4). The performance of ANN was improved when the output was close to peak flow (see Figure 3b an Figure 5). The RMSE of ANN with conveniently input layer for calibration and validation are 5.3 and 3.9, respectively. The R^2 is 0.92 for training process and is 0.89 for validating process.

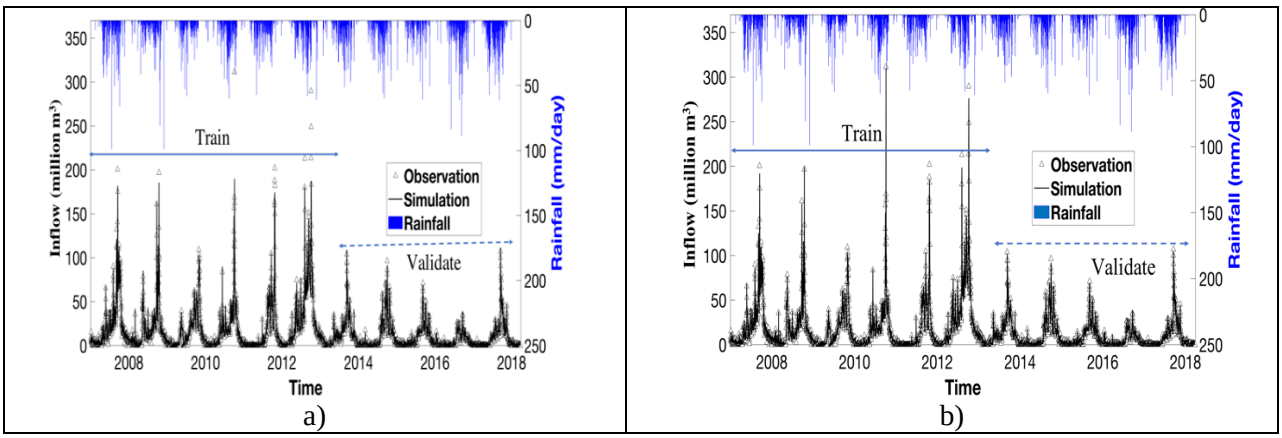

Figure 3- Results inflow of ANN a) Without conveniently input layer b) with conveniently input layer

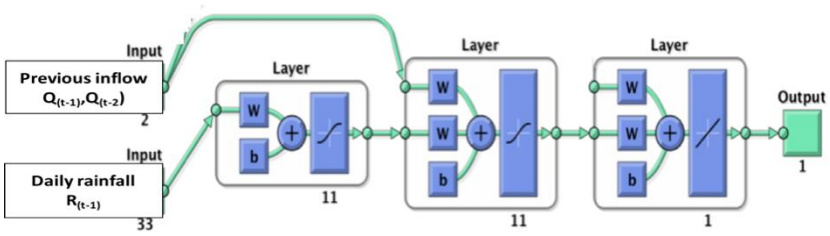

Figure 4- Structure of ANN with conveniently input layer for rainfall-runoff

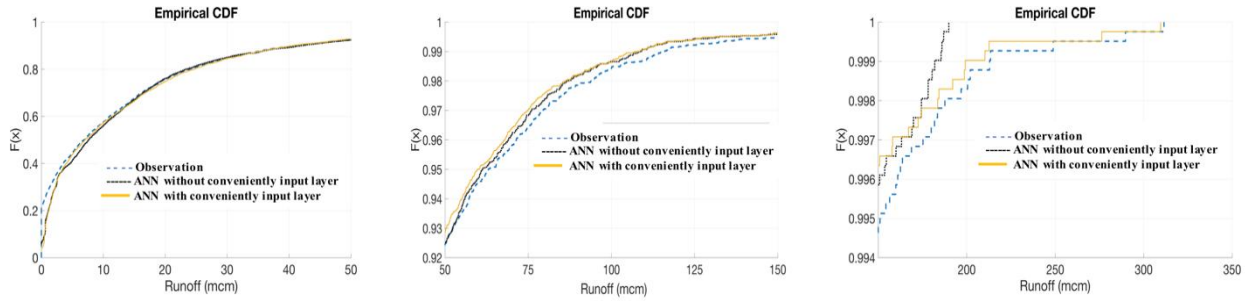

Figure 5 - Cumulative distribution function of inflows

b) Irrigation demand package

The combination of two consecutive days of capacity and inflow presented the best performance. The structure consists of 4 neurons in its hidden layer. The RMSE of calibration and validation are 5.33 mcm, and 3.912 mcm, respectively. The R^2 of calibration and validation are 0.92 and 0.95, respectively. Moreover, the cumulative distribution function curve of output is similar with the observations (see Figure 6b). Although, the simulation could not carry some immediately high release dam, the ANN is possibility to predict dam release following the current rule curve.

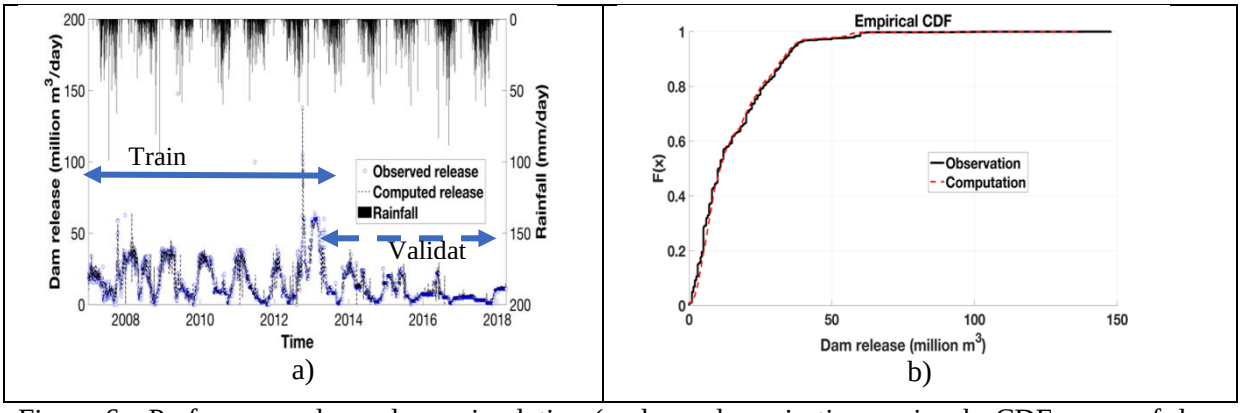

Figure 6 - Performance dam release simulation (a. dam release in time series, b. CDF curve of dam release)

c) Plant growth stage and crop area distribution

Percentage of cropland areas for irrigation area in Khamphangphet for each of growth stage, estimated using NDVI time series, showed good agreement with the percentage of report planted. For starting and harvesting period, the percentage of the cropland area seems to be smaller due to the greenness level of paddy. Area of paddy can be estimated with more accuracy during the heading time of the plant. See detail in Table 1.

Table 1 - Cultivated paddy area based on NDVI classification

Zone	Cultivated ratio (%)								Cultivation area (rai)	
									Estimated	Report
	19-Jan	4-Feb	20-Feb	8-Mar	24-Mar	9-Apr	25-Apr	Average		
1	36%	47%	48%	51%	52%	49%	36%	46%	**134,219**	
2	45%	36%	31%	43%	47%	49%	45%	42%	**98,225**	
3	48%	45%	44%	49%	50%	53%	46%	48%	**135,871**	
Total									**368,315**	**380,557**

Remarks : One rai equals to 0.16 hectare.

The growing season of rice is divided into eight phases where each phase has a different time span and also depends on crop species. In rice phenology, the greenest leaf color happens in the panicle initiation phase before the rice starts to flowering because the phonological pattern were based on EVI value or based on green index of rice.

From the pattern of time-series vegetation index, cropping period and frequency can be detected. In this paddy area, the growth will reach maximum at the panicle initiation (middle of March) where for variety rice it will take 55-60 days from germination phase (late of January) (Figure 9). The time series of EVI2 also presented the closed fluctuation with crop coefficient (Kc) which was observed and estimated in many years. Figure 7 showed the distribution of EVI2 over the irrigation area. Around middle of March, this phase will be detected by the EVI value as the highest value and then the EVI value will decrease when the rice plant started to flowering and then harvested.

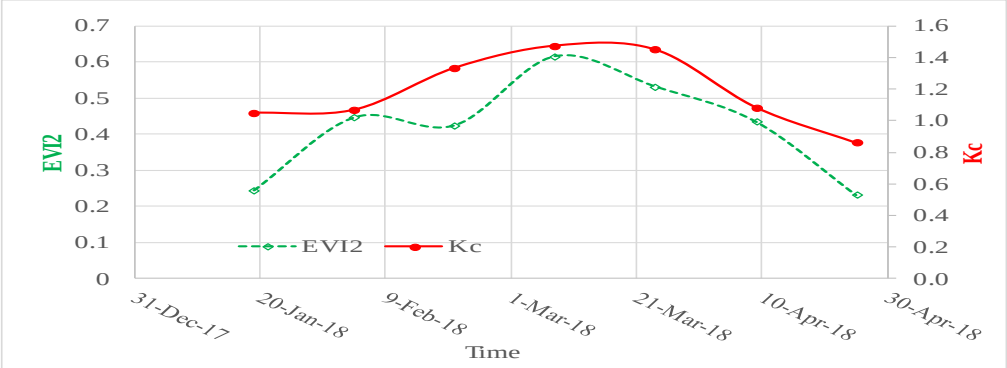

Figure 7 - Comparison of mean EVI2 values and crop coefficient (Kc)

Linear regression models of soil moisture estimation show in Figure 8a were calculated using the modified TVDI as dependent variables and observed soil moisture (from GISTDA) as the independent variable. The model constructed from TVDI index has the strong response to the actual soil moisture and likely a good ability to accurately estimate soil moisture based its high adj-R2 (0.6) and low RMSE (2%).

The function was verified by comparing observed soil moisture content (SMC) at two observed locations in Phitsanulok area with estimated SMC which was applied the function and TVDI values. Six Landsat 8 images were used to estimated TVDI and SMC at two locations. The estimated values of SMC presented a good correlation with observed values (adj-R^2 = 0.5876) (Figure 8b).

Therefore, the function of SMC which mainly based on variation of TVDI value, can be applied for other area to estimate SMC during dry season. The spatial distribution map shows the percentage of soil moisture in the Irrigation area is moderate in the mid of the dry season at around 20-30 % for bare soil and 30 to 40% for paddy fields.

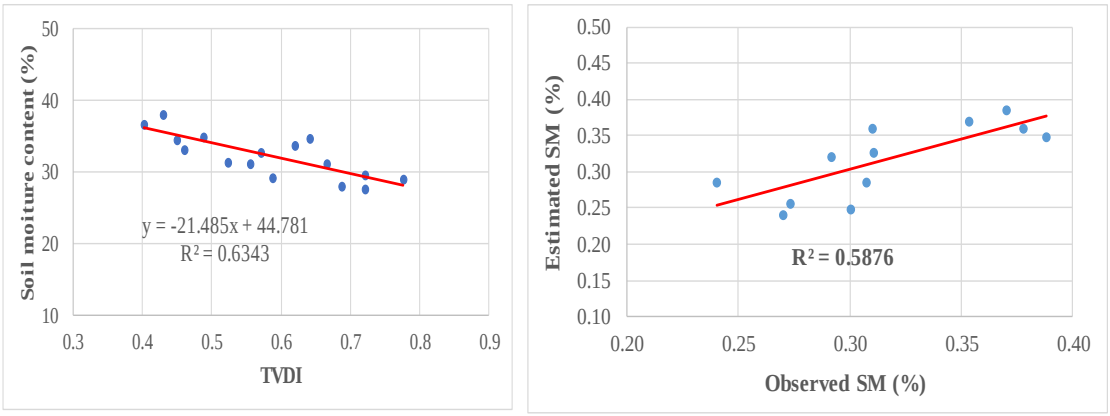

a) b)

Figure 8 - a) Correlation between TVDI coefficient and observed soil moisture content from GISTDA; b) Verification estimated SMC and observed SMC in Phitsanulok area.

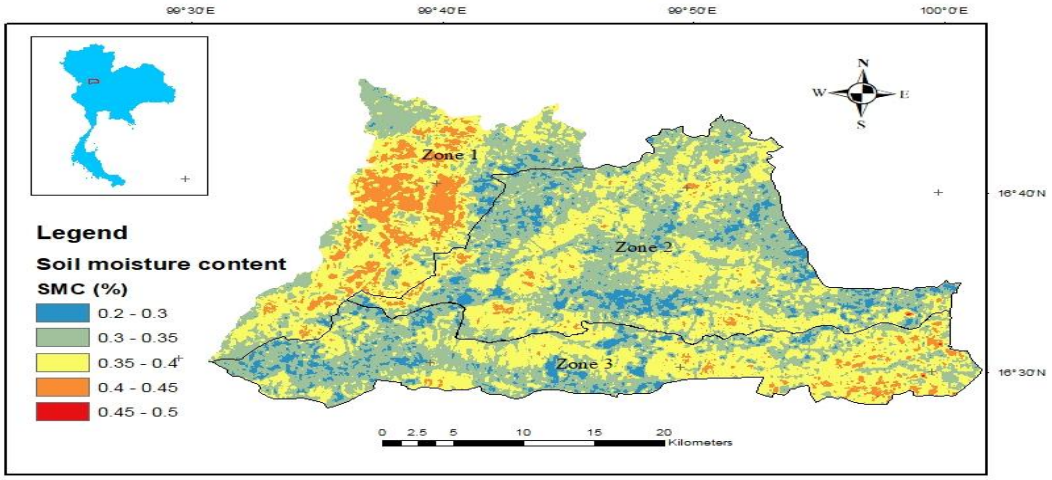

Figure 91 - Spatial distribution of soil moisture by applying the modified TVDI in the Irrigation area

Irrigation demand

Table 2 shows the estimation of the irrigation water demand of whole irrigation area. The estimated demand is highest in March due to heading and ripening period of paddy. During logging and harvesting period in April, the demand increased to about 65 MCM/month.

Table 2 - Results of irrigation water demand estimation during dry season 2018

Month	Monthly rainfall (mm)	Ce	Effective rainfall (m)	ETo (mm/d)	Kc	ET_{crop} K_c*ET_o (m)	Area (m^2)	Irrigation demand MCM
January	3.21	0.00	0.000	3.26	1.07	0.104972	5.84E+08	61.30
February	14.16	0.80	0.011	3.91	1.37	0.161092	5.84E+08	87.46
March	15.34	0.80	0.012	4.35	1.44	0.1872675	5.84E+08	102.19
April	48.61	0.80	0.039	5.01	1.01	0.151803	5.84E+08	65.94

Based on the water loss from agricultural fields due to evapotranspiration and conveyance, irrigation water demand for the command area was calculated from January to April 2018. In this study, the net irrigation water demand was computed on monthly.

Table 3 – Summary of irrigation supply-demand ratio in the year 2018

Time	Irrigation demand MCM	Water supply MCM	Net Demand - Supply MCM	Ratio of Supply/Demand	Soil moisture
Jan-18	61.30	77.5	-16.20	0.72	27%
Feb-18	87.46	60	27.46	0.51	38%
Mar-18	102.19	75	27.19	0.47	40%
Apr-18	65.94	0	65.94	0.00	30%

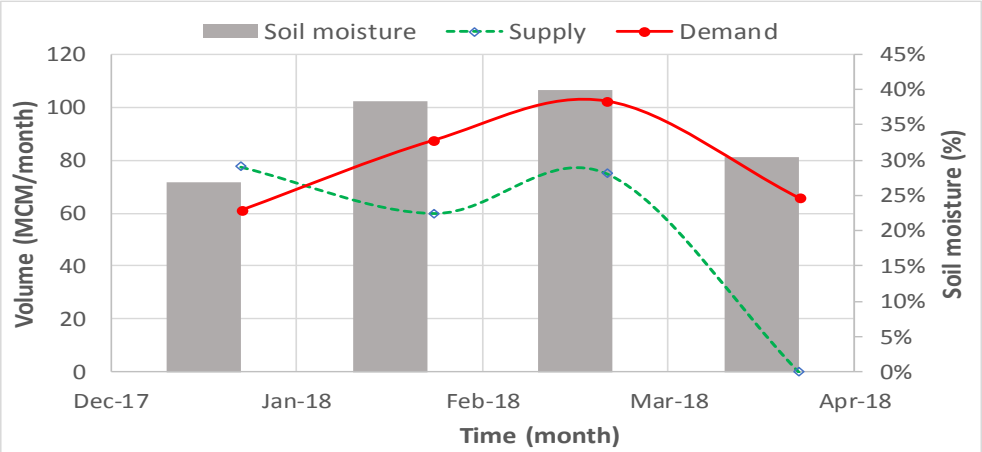

Figure 11 – Monthly amount of irrigation water demand/supply and soil moisture

Release decision making via smart system development

Previously, the dam operation is set by demand estimate from the past average record and controlled by upper and lower rule curve. With the developed rainfall-inflow-release data from ANN and soil moisture based irrigation demand, the dam release can be reoptimized with the more real time information to get up-to-dated inflow and demand figures as shown in Figure 12.

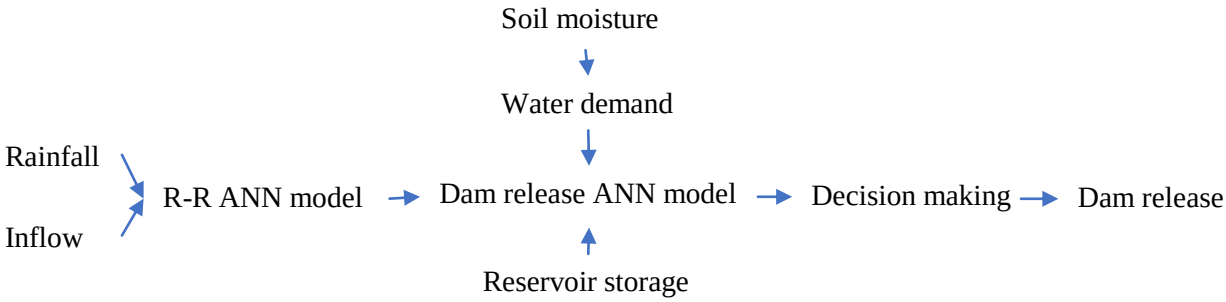

Figure 12 – Approach release decision making via smart system development

5) **Conclusions**

ANN technique can capture the inflow from rainfall data and dam release from dam storage while satellite images with ground soil moisture sensor data helped to estimate irrigation demand in near real time and accurate enough for development of smart dam operation system. The results show how smart system concept was applied and improve dam operation by using inflow estimation from ANN technique combining with irrigation demand estimation from satellite images when compared with the past procedure which is a step to develop the smart dam operation system in Thailand.

6) Acknowledgement

The authors would like to express sincere thanks to NRCT-TRF Spearhead Research Program on Water Resources Management for their research funding, thanks to RID-Thor Thong Daeng Irrigation Project, Kamphengphet Province, GISTDA for their assistances for field data provision, satellite images and to Chulalongkorn University for their working place and utility provision.

References

Alhammadi, M, and A Al-Shrouf. 2013. 'Irrigation of sandy soils, basics and scheduling. Agricultural: crop production', *InTech Book Series*.

Allen, Richard G, Luis S Pereira, Dirk Raes, and Martin Smith. 1998. 'Crop evapotranspiration-Guidelines for computing crop water requirements-FAO Irrigation and drainage paper 56', *Fao, Rome*, 300: D05109.

Celeste, Alcigeimes B, and Max %J Advances in Water Resources Billib. 2009. 'Evaluation of stochastic reservoir operation optimization models', 32: 1429-43.

Chaleeraktrakoon, Chavalit, and Anongrit Kangrang. 2007. 'Dynamic programming with the principle of progressive optimality for searching rule curves', *Canadian Journal of Civil Engineering*, 34: 170-76.

Champagne, Catherine, Tracy Rowlandson, Aaron Berg, Travis Burns, Jessika L'Heureux, Erica Tetlock, Justin R Adams, Heather McNairn, Brenda Toth, and Daniel Itenfisu. 2016. 'Satellite surface soil moisture from SMOS and Aquarius: Assessment for applications in agricultural landscapes', *International journal of applied earth observation and geoinformation*, 45: 143-54.

Chen, Shulin, Zuomin Wen, Hong Jiang, Qingjian Zhao, Xiuying Zhang, and Yan Chen. 2015. 'Temperature vegetation dryness index estimation of soil moisture under different tree species', *Sustainability*, 7: 11401-17.

De Vos, NJ, and THM Rientjes. 2005. 'Constraints of artificial neural networks for rainfall-runoff modelling: trade-offs in hydrological state representation and model evaluation', *Hydrology Earth System Sciences Discussions*, 2: 365-415.

Ehsani, Nima, Balazs M. Fekete, Charles J. Vörösmarty, Zachary D. %J Stochastic Environmental Research Tessler, and Risk Assessment. 2016. 'A neural network based general reservoir operation scheme', 30: 1151-66.

Ehsani, Nima, Charles J. Vörösmarty, Balázs M. Fekete, and Eugene Z. Stakhiv. 2017. 'Reservoir operations under climate change: Storage capacity options to mitigate risk', *Journal of Hydrology*, 555: 435-46.

Gao, Zhiqiang, Wei Gao, and Ni-Bin Chang. 2011. 'Integrating temperature vegetation dryness index (TVDI) and regional water stress index (RWSI) for drought assessment with the aid of LANDSAT TM/ETM+ images', *International journal of applied earth observation and geoinformation*, 13: 495-503.

Huntington, Thomas G. 2006. 'Evidence for intensification of the global water cycle: review and synthesis', *Journal of Hydrology*, 319: 83-95.

Jiang, Zhangyan, Alfredo R Huete, Kamel Didan, and Tomoaki Miura. 2008. 'Development of a two-band enhanced vegetation index without a blue band', *Remote Sensing of environment*, 112: 3833-45.

Kaufman, YJ, Didier Tanré, O Dubovik, A Karnieli, and LA Remer. 2001. 'Absorption of sunlight by dust as inferred from satellite and ground-based remote sensing', *Geophysical Research Letters*, 28: 1479-82.

Kim, Taesoon, Jun-Haeng Heo, and Chang-Sam Jeong. 2006. 'Multireservoir system optimization in the Han River basin using multi-objective genetic algorithms', *Hydrol Process 20*, 20: 2057-75.

Kolmogorov, Andrei Nikolaevich. 1957. "On the representation of continuous functions of many variables by superposition of continuous functions of one variable and addition." In *Doklady Akademii Nauk*, 953-56. Russian Academy of Sciences.

Lamom, Alongkorn, Thaksin Thepchatri, and Wanchai Rivepiboon. 2008. 'Heuristic algorithm in optimal discrete structural designs', *Am. J. Applied Sci*,, 5: 943-51.

Potić, Ivan, Marko Bugarski, and Jelena Matić-Varenica. 2017. "Soil Moisture Determination using Remote Sensing data for the property protection and increase of agriculture production." In *Worldbank conference on land and poverty", The World Bank, Washington DC*.

Rajurkar, MP, UC Kothyari, and UC %J Journal of Hydrology Chaube. 2004. 'Modeling of the daily rainfall-runoff relationship with artificial neural network', 285: 96-113.

Rittima, Areeya. 2009. 'Hedging policy for reservoir system operation: a case study of Mun Bon and Lam Chae reservoirs', *Kasetsart J (Natural Science)*, 43: 833-42.

Sandholt, Inge, Kjeld Rasmussen, and Jens Andersen. 2002. 'A simple interpretation of the surface temperature/vegetation index space for assessment of surface moisture status', *Remote Sensing of environment*, 79: 213-24.

Schirmbeck, Lucimara Wolfarth. 2017. 'Understanding TVDI as an index that expresses soil moisture', *Journal of Hyperspectral Remote Sensing*, 7: 82-90.

Tospornsampan, Janejira, Ichiro Kita, Masayuki Ishii, and Yoshinobu Kitamura. 2005. 'Optimization of a multiple reservoir system operation using a combination of genetic algorithm and discrete differential dynamic programming: a case study in Mae Klong system, Thailand', *Paddy Water Environment*, 3: 29-38.

Tucker, Compton J. 1979. 'Red and photographic infrared linear combinations for monitoring vegetation', *Remote Sensing of environment*, 8: 127-50.

Automatic recognition of alertness and drowsiness from EEG by an artificial neural network', 24: 349-60.